

# A Population-Based Ultra-Widefield Digital Image Grading Study for Age-Related Macular Degeneration–Like Lesions at the Peripheral Retina

Imre Lengyel, PhD,<sup>1</sup> Adrienne Csutak, MD, PhD,<sup>2,3</sup> Daniela Florea, PhD,<sup>1,2</sup> Irene Leung, BA,<sup>2</sup> Alan C. Bird, MD,<sup>1</sup> Fridbert Jonasson, MD,<sup>4</sup> Tunde Peto, MD, PhD<sup>2</sup>

**Purpose:** Our understanding of the relevance of peripheral retinal abnormalities to disease in general and in age-related macular degeneration (AMD) in particular is limited by the lack of detailed peripheral imaging studies. The purpose of this study was to develop image grading protocols suited to ultra-widefield imaging (UWFI) in an aged population.

**Design:** A cross-sectional study of a random population sample in which UWFI was introduced at the 12-year review of the Reykjavik Eye Study in Iceland.

**Participants:** Five hundred seventy-six subjects 62 years of age or older.

**Methods:** Ultra-widefield (up to 200°) color and autofluorescence images were obtained using the Optos P200CAF laser scanning ophthalmoscope (Optos plc, Dunfermline, Scotland). The images were graded at Moorfields Eye Hospital Reading Centre primarily based on the International Classification for AMD. Macular and peripheral changes were graded using a standardized grid developed for this imaging method.

**Main Outcome Measures:** Presence or absence of hard, crystalline, and soft drusen; retinal pigment epithelial changes; choroidal neovascularization (CNV); atrophy; and hypoautofluorescence and hyperautofluorescence were graded in the peripheral retina.

**Results:** Of the eyes examined, 81.1% had AMD-like changes in the macula alone (13.6%), periphery alone (10.1%), and both periphery and macula (57.4%). There was no AMD-like CNV or pigment epithelial detachment in the periphery except in those cases in which these clearly originated from the macula. Seven patients had AMD-like atrophy in the periphery without end-stage disease in the macula. One patient with end-stage disease in the macula had normal periphery results on the color images. While analyzing the eyes, we detected pathologic appearances that were very reliably identified by graders.

**Conclusions:** Phenotyping the retinal periphery using the categories defined by the International Classification confirmed the presence of wide-ranging AMD-like pathologic changes even in those without central sight-threatening macular disease. Based on our observations, we propose here new, reliably identifiable grading categories that may be more suited for population-based UWFI. *Ophthalmology* 2015;■:1–8 Crown Copyright © 2015 Published by Elsevier Inc. on behalf of American Academy of Ophthalmology. This is an open access article under the CC BY-NC-ND license (<http://creativecommons.org/licenses/by-nc-nd/4.0/>).



Supplemental material is available at [www.aaojournal.org](http://www.aaojournal.org).

Early and late age-related macular degeneration (AMD) show distinct topographic patterns of change in the outer retina. Although the diagnosis relies on changes in the macula, there are many age-related changes in the peripheral fundus<sup>1,2</sup> that may be associated with certain subtypes of AMD such that recording peripheral changes may be important in generating more accurate AMD phenotypes, which then could guide treatment strategies. Wide-field imaging protocols such as 5- or 7-field images were generated in the past,<sup>3,4</sup> but most publications are studies of diabetic retinopathy, not AMD. These imaging protocols allowed the visualization of approximately 75°

fields. Ultra-widefield imaging (UWFI) of the retina of up to 200° is now available through the use of Optos P200CAF, a scanning laser ophthalmoscope (Optos Plc, United Kingdom). Conventional and UWFI grading in the macula showed excellent correlation<sup>5</sup>; therefore, the P200CAF can be used to detect reliably central changes such as drusen, pigmentary changes, choroidal neovascularization (CNV), and geographic atrophy (GA), implying that this imaging method could be used for grading for changes outside the macular region. Herein we present grading protocols and the results of UWFI of patients participating in the 12-year review of the Reykjavik Eye Study. As far as we

know, this is the first time UWFI was used in a population-based study of AMD-like changes that analyzes color as well as autofluorescent peripheral images.

## Methods

The Reykjavik Eye Study included a random sample from the Reykjavik population census of persons 50 years of age and older in 1996, in which 1045 persons participated. All underwent an eye examination and stereo fundus photography using films.<sup>6</sup> In 2008, a 12-year review was conducted in which 576 persons participated, representing 73% of the survivors. Participants of this review were photographed using the P200CAF, an ultra-widefield (200°) scanning laser ophthalmoscope that was operated by an imaging team provided by Optos (Optos plc, Dunfermline, Scotland) and supervised by the Moorfields Eye Hospital Reading Centre. In general, imaging with the Optos P200CAF does not require dilation, although through the patients' involvement in other examinations in the Reykjavik Eye Study, their pupils were all dilated using Mydracyl 1% (Alcon, Fort Worth, TX) and phenylephrine hydrochloride 10% (Akron, Lake Forest, IL). The P200CAF uses red (633-nm) and green (532-nm) lasers to generate color images that are reflected off a large concave elliptical mirror. The resulting images are displayed as red only, green only, and a combination of red and green false-color images. The area to grade on a UWFI is significantly larger than the area covered by a classical fundus image (Fig 1A). The P200CAF also is capable of obtaining autofluorescent images by using the green (532-nm) laser for excitation and recording the autofluorescent-emitted signal by a bright-band detector (570–780 nm; Fig 1D, F, H). Each image had a resolution of 3000 × 3000 pixels.

The tenets of the Declaration of Helsinki were followed. Ethical approvals were obtained from the Icelandic Data Protection Authority and the Icelandic National Bioethics Committee. Signed informed consent was obtained from each participant. The digital images were sent to the Moorfields Eye Hospital Reading Centre with a unique identification number displayed on all photographs. These identification numbers were used to identify patients and grading records in the Reykjavik Eye Study.

Images were graded without access to clinical information using the Optos V2 vantage DX review software provided with the camera. Using this software, the grader was allowed to modify  $\gamma$  on the images, but no other modification was allowed. The review software was modified to allow the automatic fitting of an ultra-widefield grid (Fig 1B) that was based on the original definition of a standard macular grid (zones 1–3). Concentric rings were defined based on the distance between the centers of the optic nerve head and the foveola (defined to be 4500  $\mu\text{m}$ ) using the prespecified macular grid of the International Classification and the Age-Related Eye Disease Study.<sup>7,8</sup> This definition was necessary to be able to compare zones 1 through 3 on UWFI and conventional 45° images. Macular comparison showed no substantial differences in disease severity, as reported earlier.<sup>5</sup> In addition to the macular zones, 2 further zones were created: zone 4 for the mid periphery (with a diameter of 11 000  $\mu\text{m}$ ) and zone 5 for the far periphery—essentially all areas outside zone 4 (Fig 1B). These zones were generated on unprojected (without correction for possible peripheral distortion) images because this function was not available at the time of the grading. It is also important to note that there was no precedent of grading peripheral retinal UWFI changes at the time of this grading, and therefore these zones (Fig 1B, zones 4 and 5) were arbitrary. The zones were subdivided into 4 quadrants through the center of the fovea (Fig 1B), creating temporal and nasal superior quadrants and temporal and nasal inferior quadrants. Only abnormalities resembling early and late AMD were graded.

Detailed grading of all images was conducted by the same person using the categories of the International Classification<sup>7</sup> in all quadrants and zones: hard, crystalline, and soft drusen; retinal pigment epithelial changes; pigment epithelial detachment; atrophy; and CNV were graded. On autofluorescence (AF) images, hyperautofluorescence and hypoautofluorescence changes were recorded. Incidental findings were noted on the grading form. Because this was a novel imaging method, there was no grading scheme or trained grader available at the start of the study. Therefore, extensive training and validation of the detailed grading protocol took place before the grader (A.C.) for this study was certified. As such, there was no intergrader variability calculated for the detailed grading. Intraobserver agreement was calculated after 20% of images, randomly selected, were regraded after 14 days by the same certified grader (A.C.) and exact agreement and  $\kappa$  statistics were calculated. A new, simplified grading protocol, based on the overall assessment of the entire color images, was developed after the detailed grading by the authors. Two graders (I.L. and D.F.) were trained to use this simplified grading protocol, and this time, intergrader variability also was calculated.  $\kappa$  Statistics were used to determine concordance between appearance of changes between zones and quadrants and symmetry between the 2 eyes. The  $\kappa$  statistic was interpreted as follows: <0, no agreement; 0 to 0.2, slight agreement; 0.21 to 0.40, fair agreement; 0.41 to 0.60, moderate agreement; 0.61 to 0.8, substantial agreement; and >0.81, almost perfect agreement.<sup>9</sup> Statistical analysis was performed using Stata software version 9.0 (StataCorp LP, College Station, TX).

## Results

### Comparison of Macular and Peripheral Abnormalities

**Color Images.** At the 12-year review, the 576 participants examined were 62 years of age or older. Median age was 72 years. Main reasons for the loss of participants were death during the 12 years since the baseline study, accounting for 42.1% of those 50 to 59 years of age at baseline and 77.3% of those 70 to 79 years of age at baseline. Other reasons included frailty and immobility: 16% of those 50 to 59 years of age at baseline to 28.1% of those 70 to 79 years of age at baseline, despite offering free transportation to the clinic. Gender distribution among those attending and those not attending was similar. Of the total 1152 eyes (576 participants), 14 eyes (7 participants; 1.2%) could not be imaged by the Optos P200CAF because of fatigue (this imaging method was station 10 of the 11-station study) or inability to open eyes. The UWFI of the remaining 1138 eyes (569 participants) were of sufficiently good quality for grading.

Based on a simplified clinical grading that assessed only the presence or absence of abnormalities, 215 eyes (18.9%) had no observable abnormality either in the macula (zones 1–3) or periphery (zones 4 and 5) and 653 eyes (57.4%) had abnormalities at both locations (Table 1). Lesions only in the macula were present in 155 eyes (13.6%), and lesions only in the periphery were present in 115 eyes (10.1%; Table 1). The concordance between clinical grading in the left and the right eyes was moderate for both the macula ( $\kappa = 0.57$ ;  $P < 0.001$ ) and the periphery ( $\kappa = 0.45$ ;  $P < 0.001$ ). The concordance in clinical grading between the macula and periphery within the same eye was fair for both right ( $\kappa = 0.39$ ;  $P < 0.001$ ) and left ( $\kappa = 0.32$ ;  $P < 0.001$ ) eyes. This grading protocol was devised by the authors, one of whom was trained as a grader (A.C.). Ten percent of the images were reviewed by the clinical lead (T.P.) after random selection generated by an independent third-party statistician with no



**Figure 1.** Representative images taken by the Optos P200CAF ultra-widefield laser scanning ophthalmoscope: (A,C,E,G) false-color images, (B,D,F,H) autofluorescent images.

Table 1. Basic Characteristics of the 1138 Eyes in the Reykjavik Eye Study Phenotyped by Changes on Color Images

Macula Color	Periphery Color	
	Normal	Pathologic Features
Normal	215 (18.9%)	115 (10.1%)
Pathologic features	155 (13.6%)	653 (57.4%)

Percentages of totals are in parentheses.

access to the grading data or to the images. Given that we had only 1 trained grader, only intragrader reliability was measured. Intragrader reliability was high in all categories ( $\kappa > 0.81$ ;  $P < 0.001$ ). Temporal drift was not graded because all image analysis was finalized within 4 months.

Table 2 shows the cross-tabulation of the macular and peripheral phenotypes. No clearly definable pigment epithelial detachment could be seen in the periphery. Of the 155 eyes that were graded as normal in the periphery, 154 had drusen and 1 had a mixed phenotype (both CNV and GA were present in the macula and it was not possible to decide the nature of the original lesion). Of those that were normal in the macula, 9 had retinal pigment epithelial changes, 105 had drusen, and 1 had outer retinal atrophy at the periphery. Almost half of the eyes had drusen both in the macula and in the periphery ( $n = 560$ ; 49.2%). Of those with end-stage disease in the macula ( $n = 34$ ), all except 1 had visible lesions in the periphery. Choroidal neovascularization in the macula ( $n = 13$ ) was associated with drusen or mixed CNV and atrophy at the periphery, but no CNV-only case was seen in the periphery. Of the 12 GA cases in the macula, 8 had drusen only and 4 had atrophy in the periphery. Macular pigment epithelial detachment was associated with drusen only in the periphery, whereas the 7 eyes with mixed macular phenotype (CNV and GA together) were associated with no visible changes in 1 eye, drusen only in 5 eyes, and atrophy in 1 eye.

**Autofluorescence Images.** Ultra-widefield AF images also were acquired from the 576 participants. Of the total of 1152 AF images, 28 (2.4%) were considered missing because of the participant's inability to tolerate a second imaging as a result of fatigue or inability to open eyes. The UWFI of the remaining 1124 eyes were sufficiently good quality for grading AF in the periphery. Overall, 39 eyes had lesions in the macula (laser burns, disciform scar, or branch retinal vein occlusion on color images) that made AF grading inconclusive. These were excluded from the analysis.

Table 3. Basic Characteristics of the 1138 Eyes in the Reykjavik Eye Study Phenotyped by Autofluorescent Changes

Macula Autofluorescence	Periphery Autofluorescence	
	Normal	Pathologic Features
Normal	738 (67.7%)	202 (18.4%)
Pathologic Features	70 (6.4%)	81 (7.4%)

Percentages of totals are in parentheses.

Based on a simplified grading scheme, termed here as clinical grading, that assessed the presence or absence of AF abnormalities, 738 eyes (67.7%) had no observable abnormality either in the macula (zones 1–3) or periphery (zones 4 and 5) and 81 (7.4%) had abnormalities at both locations (Table 3). Autofluorescence abnormality only in the macula was present in 70 (6.4%), and AF abnormality only in the periphery was present in 201 eyes (18.4%; Table 3).

The concordance between clinical AF grading in the left and the right eyes was moderate for both the macula ( $\kappa = 0.61$ ;  $P < 0.001$ ) and the periphery ( $\kappa = 0.48$ ;  $P < 0.001$ ). The concordance in clinical AF grading between the macula and periphery within the same eye was fair for both the right eye ( $\kappa = 0.25$ ;  $P < 0.001$ ) and left eye ( $\kappa = 0.22$ ;  $P < 0.001$ ). Intragrader reliability was high in all categories ( $\kappa > 0.81$ ;  $P < 0.001$ ).

### Detailed Peripheral Grading

For further analysis, zones 4 and 5 were subdivided into 4 quadrants for better definition of the spatial distribution of abnormalities (Fig 2; details are in Table 4, available at [www.aaojournal.org](http://www.aaojournal.org)). Based on size on the unprojected images, drusen were hard ( $<125 \mu\text{m}$ ), soft ( $>125 \mu\text{m}$ ), or crystalline. Hard drusen were distributed across the retinal periphery but were most common in the supranasal quadrant in zone 5. The least hard drusen were seen in the inferotemporal quadrant. Soft drusen were most common in the superior quadrants, with a similar level of deposition in both zones 4 and 5 here. Retinal pigment epithelial changes were found mainly in zone 5, with a trend for the superior quadrants. Both hypoautofluorescent and hyperautofluorescent changes were observed in higher prevalence nasally than temporally, especially in zone 5. For crystalline drusen, CNV, and atrophy the numbers are too small to draw conclusions about distribution.

Table 2. Detailed Macular and Peripheral Grading Cross Tabulation

Macula	Periphery				
	Normal	Retinal Pigment Epithelium Changes	Drusen Only	Mixed	Atrophy
Normal	215 (18.9%)	9 (0.8%)	105 (9.2%)	0 (0%)	1 (0.1%)
Drusen only	154 (13.5%)	51 (4.5%)	560 (49.2%)	0 (0%)	9 (0.8%)
GA	0 (0%)	0 (0%)	8 (0.7%)	0 (0%)	4 (0.4%)
PED	0 (0%)	0 (0%)	2 (0.2%)	0 (0%)	0 (0%)
CNV	0 (0%)	0 (0%)	11 (1.0%)	2 (0.2%)	0 (0%)
Mixed	1 (0.1%)	0 (0%)	5 (0.4%)	0 (0%)	1 (0.1%)

CNV = choroidal neovascularization; GA = geographic atrophy; PED = pigment epithelial detachment. Percentages of totals are in parentheses.

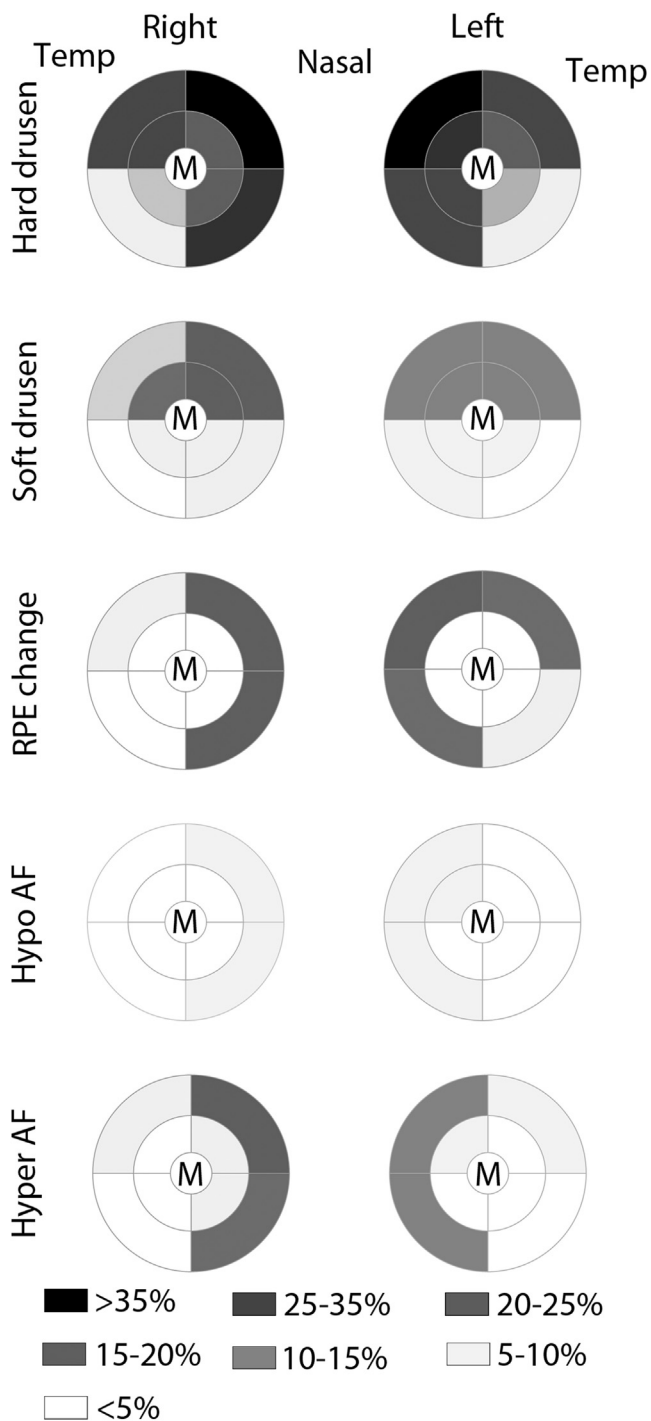


**Figure 2.** Visual representation of detailed grading of peripheral retinal lesions in zones 4 and 5 broken down into quadrants in both right and left eyes. The color scheme represents the ranges of changes represented as the percentage of all eyes. Values for crystalline drusen, choroidal neovascularization, and atrophy were very low and are depicted only in [Table 4](#) (available at [www.aaojournal.org](http://www.aaojournal.org)). AF = autofluorescence; M = macula; RPE = retinal pigment epithelium; temp = temporal.

The symmetry of changes between different categories and quadrants in the left and right eyes ranged between fair and substantial. The most consistent symmetry was detected for atrophy in all quadrants of zone 5 ( $\kappa = 0.72\text{--}0.75$ ;  $P < 0.001$ ), with wider

variability in zone 4 ( $\kappa = 0.39\text{--}0.80$ ;  $P < 0.001$ ). The symmetry for hard drusen was moderate ( $\kappa = 0.46\text{--}0.58$ ;  $P < 0.001$ ) in zone 4 and fair to moderate in zone 5 ( $\kappa = 0.25\text{--}0.52$ ;  $P < 0.001$ ). In the case of soft drusen, the symmetry was fair ( $\kappa = 0.32\text{--}0.45$ ;  $P < 0.001$ ) for all quadrants and zones. Pigmentary changes showed fair symmetry in zone 4 ( $\kappa = 0.22\text{--}0.30$ ;  $P < 0.001$ ) and moderate symmetry in zone 5 ( $\kappa = 0.50\text{--}0.64$ ;  $P < 0.001$ ). Symmetry for hypoautofluorescence was moderate ( $\kappa = 0.36\text{--}0.63$ ;  $P < 0.001$ ) and symmetry for hyperautofluorescence was fair to moderate ( $\kappa = 0.16\text{--}0.47$ ;  $P < 0.001$ ) for all quadrants and zones. Numbers for other abnormalities were too low to obtain valid comparisons.

Based on the grading data, it seems that the supranasal quadrant is the most affected in this patient population ([Fig 2](#)). Therefore, we determined the possible correlation between the appearance of an abnormality in the supranasal quadrant with the same abnormality in the other quadrants within zones 4 or 5. The best correlation was found between the supranasal and inferonasal quadrants for all categories ( $\kappa = 0.66\text{--}0.87$ ;  $P < 0.001$ ) except for soft drusen, where the best correlation was between the supranasal and superotemporal quadrants ( $\kappa = 0.48\text{--}0.78$ ;  $P < 0.001$ ), supporting the findings shown in [Figure 2](#) (and [Table 4](#), available at [www.aaojournal.org](http://www.aaojournal.org)).

Next we determined whether the appearance of a certain lesion in supranasal zones 4 or 5 was associated with the appearance of any other type of lesion in the same quadrant. We found mainly fair correlation between most categories ( $\kappa = 0.21\text{--}0.40$ ;  $P < 0.001$ ). The only exception was the almost perfect correlation between hypoautofluorescence and hyperautofluorescence in zone 4 ( $\kappa = 0.82$ ;  $P < 0.001$ ). The correlation between the appearance of a lesion in zones 4 and 5 showed a fair correlation ( $\kappa = 0.21\text{--}0.40$ ;  $P < 0.001$ ) except for soft drusen, where there seems to be a moderate correlation ( $\kappa = 0.53$ ;  $P < 0.001$ ), and for atrophy, where the correlation is poor ( $\kappa < 0$ ;  $P < 0.001$ ).

### Novel Grading Categories

Following the detailed grading above, specific phenotypic patterns emerged that could not be assigned to the previously described quadrants and zones ([Fig 3](#)). We found that 10.6% of all eyes contained large fields of peripheral hard drusen (labelled as PHDF on [Fig 3A, B](#)). The most prevalent peripheral lesion we termed *peripheral reticular degeneration*, with its characteristic pigmentary changes (labelled as PRD on [Fig 3G, H](#)), that was associated with 18.3% of the eyes. Drusen deposition located next to the arcade vessels were present in 5.7% (labelled as AD on [Fig 3E, F](#)), and a peripheral soft drusen field was present in 2.5% of the eyes (labelled as PSD on [Fig 3C, D](#)). Overall, 28.5% of the eyes had at least 1 and 7.7% had more than 1 of the new peripheral grading categories. The most important observation with these grading categories was that there was no significant disagreement between 2 independent observers ( $\kappa > 0.95$ ;  $P < 0.05$  for all categories).

### Discussion

Ultra-widefield images previously have not been used to grade population-based peripheral retinal changes associated with early or late AMD, although the presence of pathologic abnormalities up to the ora serrata has been well described.<sup>2,10</sup> Here we graded UWFI based on the International Classification<sup>7</sup> and report AMD-like abnormalities in the periphery on both color and AF images. These changes are associated with specific geographic location. During detailed grading, it emerged that there are patterns of

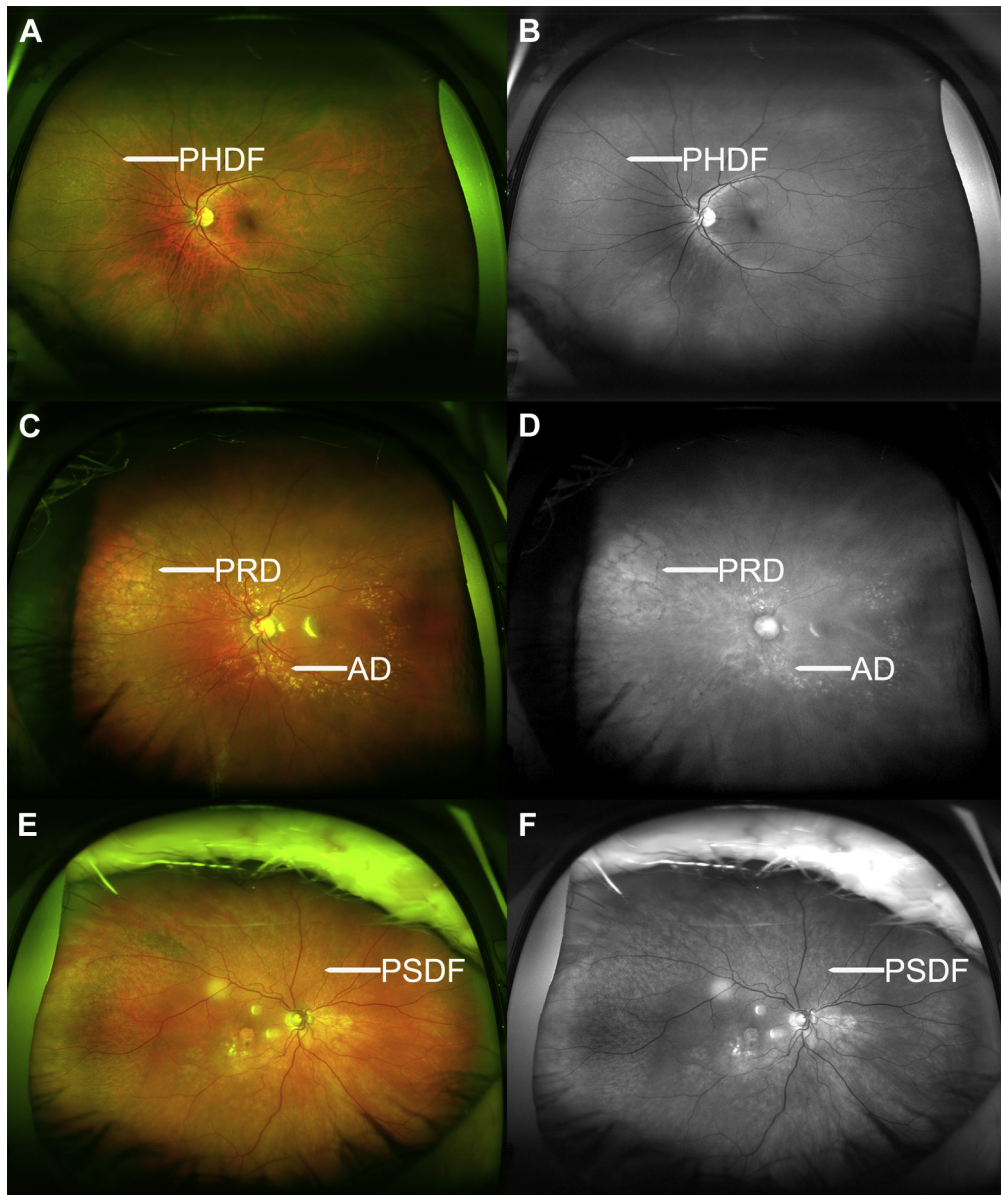


**Figure 3.** Representative images for the suggested new peripheral retinal phenotypes: (A, C, E) color images and (B, D, F) red-free images. AD = arcade drusen; PHDF = peripheral hard drusen field; PRD = peripheral reticular degeneration; PSDF = peripheral soft drusen field.

abnormalities that do not rely on zones and quadrants and are highly reproducible in grading, and thus could be used for grading peripheral retinal phenotypes.

Comparison of grading of macular abnormalities on images obtained with the Optos P200CAF with non-stereoscopic conventional digital fundus images (45°) showed no substantial differences between grading for AMD in the macula.<sup>5</sup> These Optos P200CAF images were gradable in the macula, even those that fell short of grading standards on conventional fundus images.<sup>5</sup> This was because of the capacity of laser beams to overcome problems with media opacities<sup>11,12</sup> and have higher resolution in terms of sharpness and contrast<sup>13</sup> than conventional color images. Because of these factors, only 1.2% of the

patients could not be imaged in this study; that was the result of noncompliance and not difficulty with the imaging itself. This built confidence in using UWFI for grading AMD-like changes outside of the macula.

Throughout the grading of the peripheral retina, there were several issues that needed to be addressed. Graders had to learn to appreciate artifacts related to the broad depth of focus of this device—such as the presence of eyelids, eyelashes, and floaters; the optics and the haptics of the intraocular lens; or lens opacities—and the fact that the images, because they are generated by green and red laser lights rather than the more widely used white light illumination, are less familiar to graders in the first instance (examples are shown on Figs 1 and 3). Occasionally, more than 1 image of

the same eye had to be graded because of blinking or difficulty opening the eyelids. The reported distortion at the peripheral retina<sup>14</sup> also posed issues in how this may affect the perceived size of drusen and the grading of quadrants, especially in zone 5. However, we found that most of these aspects can be overcome or minimized with practice and good imaging techniques and believed that distortions are unlikely to affect the overall conclusions of this study. How, if at all, previously reported problems with the Optos P200, an earlier device, in the misdiagnosis and artefacts related to broad depth of field<sup>15,16</sup> may affect far peripheral grading for early and late AMD using Optos P200CAF images will need to be evaluated in follow-up studies.

Using flat-mount cadaveric eyes, it has been shown that pathologic changes external to the RPE are often masked by the presence of the RPE.<sup>10</sup> Therefore, the peripheral retina changes seen in this UWFI study are likely to be underestimates. Whether these hidden changes become clinically evident with time needs to be evaluated in follow-up studies. Masking effects in the superior and inferior periphery by the eyelids and eyelashes and loss of image quality may add to this underestimation. The loss of imaging fields was variable between participants (Fig 1) but was not estimated here. Some of the loss could be overcome by generating steered images. However, this was not attempted in this study because of the need to image a large volume of patients (approximately 100 participants in 1 day) and the time constraints resulting from UWFI being only 1 of the 11 examination stations in this study. By overcoming the problems associated with loss of field and correcting for the warping of images, new ultra-widefield ophthalmoscopes will lead to a more streamlined, more accurate, and faster imaging of AMD-like abnormalities at the peripheral retina in large populations.

The fact that most affected eyes had changes at both the macula and the periphery shows that the abnormalities leading to AMD may not be restricted only to the macula. To understand the significance of peripheral retina changes to disease progression, it will be necessary to review these patients from time to time. The observation that there are eyes with only macular or only peripheral changes (Table 1) reflects the diversity of AMD-like changes that is likely to be related to the various risk factors.

Overall, we can say confidently that in the Reykjavik Eye Study population, peripheral—especially far peripheral—drusen deposition, pigmentary changes, and hypoauto-fluorescent and hyperauto-fluorescent changes are abundant in most eyes. However, the number of eyes with crystalline drusen, CNV, or atrophy were too few to ascertain with confidence the spatial distribution of these categories. The intriguing finding that pathologic changes show specific special distributions (Fig 2) will require further investigations. For example, it will be interesting to learn why there were more numerous hard drusen deposited nasally with a preference for the superior quadrant (Fig 2) and why soft drusen were enriched in the superior quadrants (Fig 2). The relationships between the appearance of abnormalities in zones 4 and 5 are not strong ( $\kappa < 0.60$ ), suggesting that their development at

these different eccentricities are probably not closely related, and this gives support to our choice of subdivision of the peripheral retina (Fig 1B). Overall, lesions were most prevalent in zone 5 (Fig 2), an area known to be prone to ophthalmoscopic abnormalities throughout life. What anatomic features determine the regional distribution of changes in the periphery is unknown. One potential contributor may be the nature of the choroidal vasculature and the associated metabolic supply.<sup>17,18</sup>

It is intriguing that the supranasal quadrant is most prone to pathologic changes in this population. One explanation may be related to photo-oxidative damage triggered by solar ultraviolet radiation that arrives from a lower zenith angle in Iceland than most other countries. The lower zenith angle had been associated with an increased risk for cortical cataract development in the superior quadrant in this population.<sup>19</sup> Therefore, UWFI of other aging populations will be needed to evaluate whether the same predilection is true in other communities.

Although detailed grading revealed some intriguing special differences, this grading may not be easy to implement in a clinical environment. However, during the original grading of these eyes, several characteristic patterns emerged (Fig 3). These were not associated with zones or quadrants but were well recognizable, easy to grade reproducibly, and could be easily implemented in the clinic. These phenotypes were associated with vast areas of the peripheral retina and were distinct from macular changes. Their association with early or late AMD in the macula should be investigated in follow-up studies. However, we do not yet know whether these phenotypes are clinically relevant.

In summary, peripheral retina grading may be important for the fuller understanding of the development and progression of AMD and potentially other diseases.<sup>20</sup> Whether progression of peripheral abnormalities may be associated with the development or progression of macular changes remains to be evaluated by follow-up studies. Because UWFI is becoming more widespread, we soon will be able to see whether peripheral retinal changes influence the outcome of AMD and whether the results presented here can be reproduced in other populations.

**Acknowledgments.** The authors thank the participating patients, the Optos clinical research team (Douglas Anderson, Anne-Marie Cairns, David Cairns, Paul Donnelly, and Dana Keane), and the medical staff at Landspítali University Hospital, Reykjavik, Iceland, for their professional support.

## References

1. Bell FC, Stenstrom WJ. *Atlas of the Peripheral Retina*. Philadelphia: Saunders; 1983.
2. Flinn JM, Kakalec P, Tappero R, et al. Correlations in distribution and concentration of calcium, copper and iron with zinc in isolated extracellular deposits associated with age-related macular degeneration. *Metallomics* 2014;6:1223–8.
3. Chow SP, Aiello LM, Cavallerano JD, et al. Comparison of nonmydriatic digital retinal imaging versus dilated ophthalmic examination for nondiabetic eye disease in persons with diabetes. *Ophthalmology* 2006;113:833–40.

4. Seddon JM, Reynolds R, Rosner B. Peripheral retinal drusen and reticular pigment: association with CFHY402H and CFHrs1410996 genotypes in family and twin studies. *Invest Ophthalmol Vis Sci* 2009;50:586–91.
5. Csutak A, Lengyel I, Jonasson F, et al. Agreement between image grading of conventional (45 degrees) and ultra wide-angle (200 degrees) digital images in the macula in the Reykjavik eye study. *Eye (Lond)* 2010;24:1568–75.
6. Jonasson F, Arnarsson A, Sasaki H, et al. The prevalence of age-related maculopathy in iceland: Reykjavik Eye Study. *Arch Ophthalmol* 2003;121:379–85.
7. Bird AC, Bressler NM, Bressler SB, et al. An international classification and grading system for age-related maculopathy and age-related macular degeneration. The International ARM Epidemiological Study Group. *Surv Ophthalmol* 1995;39:367–74.
8. The Age-Related Eye Disease Study system for classifying age-related macular degeneration from stereoscopic color fundus photographs: the Age-Related Eye Disease Study report number 6. *Am J Ophthalmol* 2001;132:668–81.
9. Landis JR, Koch GG. The measurement of observer agreement for categorical data. *Biometrics* 1977;33:159–74.
10. Lengyel I, Tufail A, Hosaini HA, et al. Association of drusen deposition with choroidal intercapillary pillars in the aging human eye. *Invest Ophthalmol Vis Sci* 2004;45:2886–92.
11. Kirkpatrick JN, Manivannan A, Gupta AK, et al. Fundus imaging in patients with cataract: role for a variable wavelength scanning laser ophthalmoscope. *Br J Ophthalmol* 1995;79:892–9.
12. Neubauer AS, Yu A, Haritoglou C, Ulbig MW. Peripheral retinal changes in acute retinal necrosis imaged by ultra widefield scanning laser ophthalmoscopy. *Acta Ophthalmol Scand* 2005;83:758–60.
13. Neubauer AS, Kernt M, Haritoglou C, et al. Nonmydriatic screening for diabetic retinopathy by ultra-widefield scanning laser ophthalmoscopy (Optomap). *Graefes Arch Clin Exp Ophthalmol* 2008;246:229–35.
14. Witmer MT, Parlitsis G, Patel S, Kiss S. Comparison of ultra-widefield fluorescein angiography with the Heidelberg Spectralis(R) noncontact ultra-widefield module versus the Optos(R) Optomap(R). *Clin Ophthalmol* 2013;7:389–94.
15. Chou B. Limitations of the Panoramic 200 Optomap. *Optom Vis Sci* 2003;80:671–2.
16. Jones WL. Limitations of the Panoramic 200 Optomap. *Optom Vis Sci* 2004;81:165–6.
17. Wybar KC. Vascular anatomy of the choroid in relation to selective localization of ocular disease. *Br J Ophthalmol* 1954;38:513–7.
18. Luttj G, Bhutto I, McLeod D. Anatomy of the ocular vasculatures. In: Schmetterer L, Kiel J, eds. *Ocular Blood Flow*. Berlin, Heidelberg: Springer; 2012:3–21.
19. Sasaki H, Kawakami Y, Ono M, et al. Localization of cortical cataract in subjects of diverse races and latitude. *Invest Ophthalmol Vis Sci* 2003;44:4210–4.
20. Ritchie CW, Peto T, Barzegar-Befroei N, et al. Peripheral retinal drusen as a potential surrogate marker for Alzheimer's dementia: a Pilot study using ultra-wide angle imaging. *Invest Ophthalmol Vis Sci* 2011;52:2–11. E-Abstract 6683.

## Footnotes and Financial Disclosures

Originally received: October 25, 2014.

Final revision: March 5, 2015.

Accepted: March 6, 2015.

Available online: ■■■■ Manuscript no. 2014-1699.

<sup>1</sup> UCL Institute of Ophthalmology, University College London, London, United Kingdom.

<sup>2</sup> NIHR Biomedical Research Centre, Moorfields Eye Hospital NHS Foundation Trust and UCL Institute of Ophthalmology, London, United Kingdom.

<sup>3</sup> Department of Ophthalmology, Faculty of Medicine, University of Debrecen, Debrecen, Hungary.

<sup>4</sup> Faculty of Medicine, University of Iceland, Reykjavik, Iceland.

Presented at: Association for Research in Vision and Ophthalmology Annual Meeting, 2010 (Fort Lauderdale, FL) and in International Society for Imaging in the Eye/Association for Research in Vision and Ophthalmology Annual Meeting, 2011 (Fort Lauderdale, FL).

Financial Disclosure(s):

The author(s) have made the following disclosure(s): A.C.B.: Financial support – Optos Plc.

Supported by the Bill Brown Charitable Trust, London, England; Moorfields Eye Hospital Special Trustees, London, England; UCL Graduate School Research Projects Fund, London, England; and Mercer Fund from

Fight for Sight, London, England and the NIHR Biomedical Research Centre at Moorfields Eye Hospital NHS Foundation Trust and UCL Institute of Ophthalmology, London, England. The study was funded in part by an unrestricted grant from Optos PLC. Optos Plc participated in data collection by providing an imaging team. The authors alone are responsible for the content and writing of the paper.

Author Contributions:

Conception and design: Lengyel, Bird, Jonasson, Peto

Analysis and interpretation: Lengyel, Csutak, Florea, Bird, Jonasson, Peto

Data collection: Lengyel, Csutak, Florea, Leung, Jonasson, Peto

Obtained funding: Lengyel, Peto

Overall responsibility: Lengyel, Peto

Abbreviations and Acronyms:

**AF** = autofluorescence; **AMD** = age-related macular degeneration;

**CNV** = choroidal neovascularization; **GA** = geographic atrophy;

**UWFI** = ultra-widefield imaging.

Correspondence:

Tunde Peto, MD, PhD, Reading Centre, Department of Research and Development, Moorfields Eye Hospital NHS Foundation Trust, 162 City Road, London EC1V 2PD, United Kingdom. E-mail: [Tunde.Peto@moorfields.nhs.uk](mailto:Tunde.Peto@moorfields.nhs.uk)